Investigation of phase effects of coherent beam combining for large-aperture ultrashort ultrahigh intensity laser...

Article *in* Applied Optics · November 2015

DOI: 10.1364/AO.54.009939

CITATIONS
0

READS
48

14 authors, including:

Zexi Zhao
Huazhong University of Science and Technol...
4 PUBLICATIONS **0** CITATIONS
SEE PROFILE

Zhongyang Xu
Tsinghua University
12 PUBLICATIONS **12** CITATIONS
SEE PROFILE

applied optics

Investigation of phase effects of coherent beam combining for large-aperture ultrashort ultrahigh intensity laser systems

Ze-xi Zhao, Yan-qi Gao,* Yong Cui, Zhong-yang Xu, Ning An, Dong Liu, Tao Wang, Da-xing Rao, Ming Chen, Wei Feng, Lai-lin Ji, Zhao-dong Cao, Xue-dong Yang, and Wei-xin Ma

Shanghai Institute of Laser Plasma, 1129 Chenjiashan Road, Jiading, Shanghai 201800, China
**Corresponding author: liufenggyq@siom.ac.cn*

Received 10 August 2015; revised 9 October 2015; accepted 26 October 2015; posted 27 October 2015 (Doc. ID 247285); published 18 November 2015

Large-aperture ultrashort ultrahigh intensity laser systems are able to achieve unprecedented super-high peak power. However, output power from a single laser channel is not high enough for some important applications and it is difficult to improve output power from a single laser channel significantly in the near future. Coherent beam combining is a promising method which combines many laser channels to obtain much higher peak power than a single channel. In this work, phase effects of coherent beam combining for large-aperture ultrashort laser systems are investigated theoretically. A series of numerical simulations are presented to obtain the requirements of spatial phase for specific goals and the changing trends of requirements for different pulse durations and number of channels. The influence of wavefront distortion on coherent beam combining is also discussed. Some advice is proposed for improving the performance of combining. In total, this work could help to design a practical large-aperture ultrashort ultrahigh intensity laser system in the future.

OCIS codes: (140.3298) Laser beam combining; (220.4830) Systems design; (140.7090) Ultrafast lasers.

http://dx.doi.org/10.1364/AO.54.009939

1. INTRODUCTION

Ultrashort ultrahigh intensity laser systems are becoming more and more important due to their numerous applications in spectroscopy, material processing, secondary radiation generation, high-energy particle acceleration, advanced attosecond science, laser-based nuclear physics, and high-energy laboratory astrophysics [1,2]. Many efforts have been made to improve peak power of femtosecond sources to multi-petawatt (PW) even ten PW level [3]. However, output peak power is limited by various factors, for instance, damage threshold, thermo-optic effects, nonlinear effects, brightness of the pump source, and so on [4].

In order to reduce the impact of these traditional performance limitations, temporal and spatial scaling of the laser pulses have been demonstrated. The temporal scaling can be realized by the well-known techniques of chirped pulse amplification (CPA) [5] and optical parametric chirped pulse amplification (OPCPA) [6]. In these techniques, temporally stretched pulses are amplified so that the peak power of the pulses could be reduced considerably during amplification and nonlinear effects are mitigated. So far, for a single-channel laser system, the peak intensity has been improved to about 2×10^{22} W · cm^{-2} by using CPA [7], and it is very hard to improve significantly in the near future. For example, the peak intensity claimed for the planned single-channel laser systems Apollo10P and Vulcan10P is about 10^{23} W · cm^{-2} [8,9]. Spatial scaling, namely, coherent beam combining [10], is a method to improve the performance of ultrashort CPA systems further. A pulse is split into N beams spatially, and then the beams are amplified, respectively. Subsequently, all pulses are coherently recombined into one single beam and the peak output power is increased by a factor of N [11]. Many projects, such as the Extreme Light Infrastructure (ELI) [12] and the Exawatt Center for Extreme Light Studies (XCELS) [13] are planning to utilize this method. In these projects, it is planned to obtain about 10^{25} W · cm^{-2} peak intensity [14].

It is well known that the femtosecond pulse regime is essential to achieve the highest peak power. The coherent combining of continuous waves (CWs) and long pulsed waves, amplified in bulk, fiber and semiconductor amplifiers, has been intensively researched in the past decades. However, the short pulse has been coherently combined just recently [15]. In the ultrashort pulsed regime, the largest number of combined beams is 4 [16,17], the highest pulse energy is 100 mJ (peak power is

4 TW) [18], the highest peak intensity is 10^{20} W · cm^{-2} [19], and the shortest pulse duration is 23 fs [18,19]. However, all these results above are based on fiber or small aperture bulk amplifiers. The large-aperture ultrashort coherent beam combining has not been realized experimentally and even the theoretical analysis is minimal [20,21], although large-aperture OPCPA or CPA is considered as the most hopeful approach for a ten PW system.

In this paper, we investigate the phase effects of coherent beam combining in large-aperture ultrashort ultrahigh intensity laser systems. This research is meaningful for practical large-aperture ultrashort laser beam coherent combining. The paper is organized as follows. Section 2 presents a physical model of ultrashort pulse coherent beam combining. Numerical simulation results and some important properties are described in Section 3 and Section 4. Conclusions are drawn in Section 5.

2. THEORETICAL MODEL

Wavefront distortion is an important issue for combining large-aperture systems since it markedly affects the performance. Moreover, ultrashort pulses have wider spectra which could affect the far-field intensity distribution. Therefore, wavefront distribution and spectrum effects are two characteristics that must be considered in a model for coherent beam combining of large-aperture ultrashort ultrahigh intensity laser systems.

The electric field of ultrashort pulse can be represented as the vector summation of the electric field of different frequency components, and the electric field expression in the frequency domain is the Fourier transformation of that in time domain

$$\varepsilon(x,y,t) = \frac{1}{2\pi}\int_{-\infty}^{\infty} E(x,y,\omega)\exp(i\omega t)\mathrm{d}\omega,$$
$$E(x,y,\omega) = \int_{-\infty}^{\infty} \varepsilon(x,y,t)\exp(-i\omega t)\mathrm{d}t, \quad (1)$$

where $\varepsilon(x,y,t)$ represents the time domain expression at spatial coordinate (x,y), and $E(x,y,\omega)$ is the corresponding frequency domain expression.

In multichannel coherent beam combining, the near field distribution of the frequency component ω_1 has the following expression:

$$E_1(x,y,\omega_1) = \sum_{m=1}^{M}\sum_{n=1}^{N} E_{mn}(x,y)\exp(i\phi_{mn}(x,y))\exp(-i\omega_1 t), \quad (2)$$

where (x,y) is the coordinate of the near field, $E_1(x,y,\omega_1)$ is the near field distribution of the frequency component ω_1, and $E_{mn}(x,y)$ and $\exp(i\phi_{mn}(x,y))$ represent the amplitude and phase of each channel, respectively. Besides, $\exp(-i\omega_1 t)$ reflects the electric field varying over time for this frequency component. This paper focuses on the relationships between the performance of combining and $\phi_{mn}(x,y)$.

Assuming that the shape of the aperture of all channels is square, the shape of the aperture (as shown in Fig. 1) and the amplitude can be represented as

$$E_{mn}(x,y) = \mathrm{rect}\left(\frac{x-md_x}{w_x}\right)\times\mathrm{rect}\left(\frac{y-nd_y}{w_y}\right), \quad (3)$$

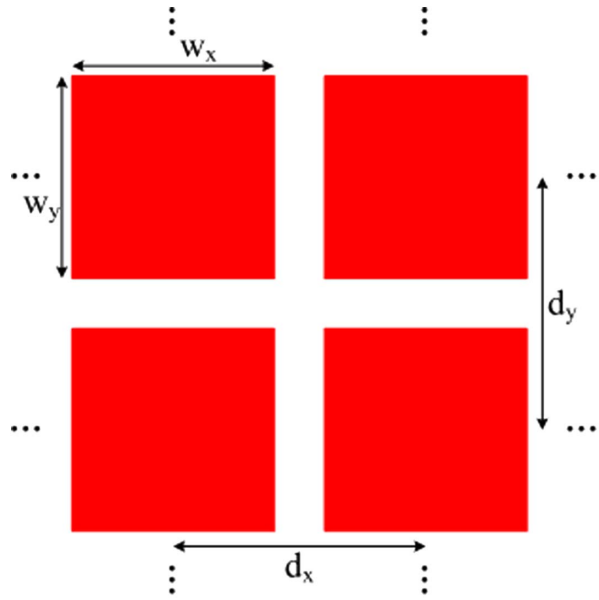

Fig. 1. Diagram of the near field of coherent beam combining.

where w and d are the beam aperture and the distance between beams, respectively, and m and n are indices of beams.

The far-field distribution of the frequency component ω_1 can be represented as

$$E_2(f_x,f_y,\omega_1) = \frac{1}{\lambda_1 f}\int E_1(x,y,\omega_1) \times \exp(-2\pi i(f_x x + f_y y))\mathrm{d}x\mathrm{d}y, \quad (4)$$

where λ_1 is the wavelength corresponding to frequency component ω_1, f is the focal length of the lens, and (f_x,f_y) is the coordinate of the focal plane.

Since the amplitudes of different frequency components are different, for each component, the focal plane electric field expression could be expressed as

$$\sqrt{I(\omega)}E_2(f_x,f_y,\omega), \quad (5)$$

where $I(\omega)$ is the spectrum distribution of an ultrashort pulse, which reflects the amplitude variation of different frequency components.

Many different frequency components propagate to the focal plane independently. The focal plane electric field is the vector summation of the far-field electric field distribution of different frequency components.

Therefore, the time domain expression of the focal plane electric field is

$$\varepsilon_2(f_x,f_y,t) = \frac{1}{2\pi}\int \sqrt{I(\omega)}E_2(f_x,f_y,\omega)\exp(-i\omega t)\mathrm{d}\omega. \quad (6)$$

We can obtain the intensity of the far field as

$$I_2(f_x,f_y) = \int_0^{\tau} |\varepsilon_2(f_x,f_y,t)|^2\mathrm{d}t, \quad (7)$$

where τ is the response time of the focal plane array.

For the case that all channels are square, Eqs. (1)–(7) are enough to discuss phase effects of coherent beam combining for large-aperture ultrashort laser systems.

To evaluate the performance of combining, we prefer to use the Strehl ratio (SR) and the encircled energy (EC) in the diffraction limit to represent peak intensity information and the concentration of energy, respectively [7]. Moreover, the Strehl ratio of encircled energy (SRdl) is also used for evaluating the concentration of energy since it may be a practical design goal in some specific cases [22]. The definition of this metric is the ratio of the power in a certain bucket for actual far-field intensity distribution and the power in the same bucket for perfectly flat wavefront far-field intensity distribution.

In order to investigate the influence of wavefront error on the performance of combining, we use the peak-to-valley (PV) of the wavefront error and the root mean square (RMS) of the wavefront error to reflect the amplitude of the wavefront error variation and the property of diffusion of the laser beam, respectively. Besides, the root mean square of the gradient of the wavefront error (GRMS) and the peak-to-valley of the gradient of the wavefront error (GPV) are used to represent the property of focusing of the laser beam [23].

3. REQUIREMENTS FOR EACH BEAM'S OWN WAVEFRONT ERROR FOR LARGE-APERTURE ULTRASHORT LASER SYSTEMS COHERENT BEAM COMBINING

Each beam's own wavefront error refers to the difference between each channel's wavefront and flat wavefront. If the wavefront of the beam is not perfectly flat, energy could not be focused on the focal point well. It decreases performance of combining significantly due to the degeneration of the peak intensity and the concentration of energy. To explain the physical meaning of our discussion more clearly, the influence of each beam's own wavefront error on two-channel large-aperture coherent beam combining is shown in Fig. 2. Figures 2(a) and 2(b) are each the beam's own wavefront in the case of SR = 0.8 and SR = 0.3, respectively. Figures 2(c) and 2(d) are corresponding normalized far-field intensity distributions for the beam combined system. It is clear that far-field intensity distribution degenerates considerably when each beam's own wavefront error becomes greater.

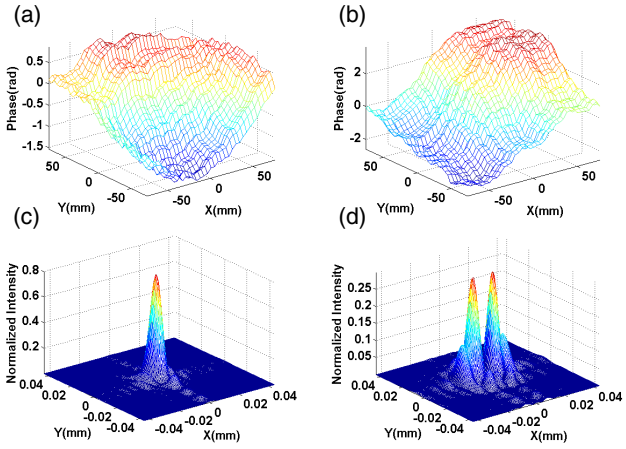

Fig. 2. (a), (b) Each beam's own wavefront for the case of SR = 0.8 and SR = 0.3, respectively. (c), (d) Corresponding normalized far-field intensity distribution for the beam combined system.

Table 1. Parameters of the Numerical Simulation Model

Parameters	Values
Central wavelength	910 nm
Pulse duration	25 fs (transform-limited)
Spectrum	Super-Gaussian (with random fluctuation, shown as Fig. 4)
Spatial distribution of each beam's near field	10th order Super-Gaussian
Distance between beams	10 mm
Aperture of each beam	150 mm ∗ 150 mm
Focal length	2 m

Based on the theoretical model discussed in Section 2, this section discusses the influence of each beam's own wavefront error on coherent beam combining. Taking into account the complexity of coherent beam combining, the Monte Carlo method is used to find the relationships between wavefront and performance of combining. Some meaningful parameters can be obtained by data fitting [24].

First, we discuss coherent beam combining of two large-aperture ultrashort laser beams. Second, the influence of pulse duration and the number of channels combined are discussed. In our numerical simulation, we set the central wavelength and the pulse duration to 910 nm and 25 fs, respectively, which are the parameters of Russian XCELS laser. The size of the British Vulcan10P laser, 150 mm ∗ 150 mm, is also used in our numerical simulation. We assume that the pulses are transform-limited. All the other parameters are set to reasonable values in terms of their time-bandwidth product. The values are listed in Table 1, with the near-field distribution presented in Fig. 3.

In order to simulate different wavefront errors, a series of random phase screens are produced by [23]

$$\phi(x,y) = \text{random}(-1,1) \otimes \exp\left\{-\left[\left(\frac{x}{sg_x}\right)^2 + \left(\frac{y}{sg_y}\right)^2\right]\right\}, \tag{8}$$

where random(−1, 1) is a uniformly distributed random number sequence in the range of −1 and 1. ⊗ represents convolution.

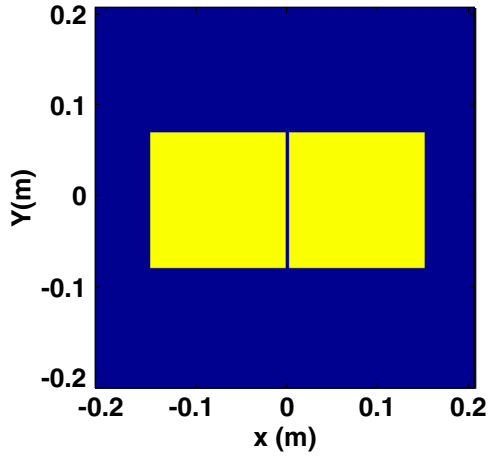

Fig. 3. Near-field distribution.

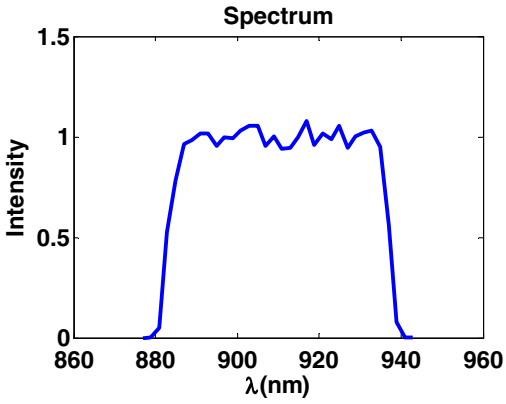

Fig. 4. Spectrum of incident light.

sg_x and sg_y are the parameters corresponding to the spatial distribution of low frequency phase. We set sg_x and sg_y in the range of 2 and 12 cm.

In order to discuss the relationships between each beam's own wavefront error and performance of combining, we set two beam phases to the same phase screen and calculate performance evaluation indices for this case. Then, the two beam phases are set to another phase screen (wavefronts of all the beams are same) and we calculate performance evaluation indices again. Repeating this process many times, we can find relationships between each beam's own wavefront error and the performance of combining by data fitting.

The results are presented in Fig. 5. The relationship between EC and SR is plotted in Fig. 5(a), and the relationship between SRdl and SR is plotted in Fig. 5(b). There is a set of approximate

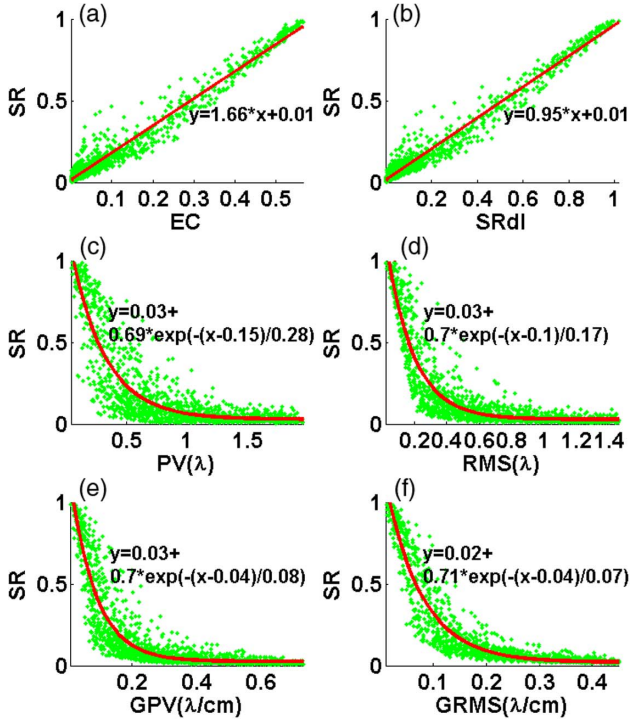

Fig. 5. (a)–(f) Effect of each beam's own wavefront error on two 25 fs transform-limited large-aperture coherent beam combining.

linear relationships among EC, SR, and SRdl. Figures 5(c)–5(f) represent the relationships between parameters (PV, RMS, GPV, and GRMS) of each beam's own wavefront and SR, respectively. Because energy could not be focused on the focal point well, SR decreases dramatically when the wavefront degenerates. Besides, we find that the performance of combining increases rapidly if we make wavefront parameters better than certain values. One possible explanation for this phenomenon is that much more subaperture can be phased together when wavefront parameters are better than these values. In this case, the size of the focal spot decreases quickly according to the above discussion. That leads to a marked increase in peak intensity.

For this system, the certain values are about PV $= 1.31\lambda$, RMS $= 0.77\lambda$, GPV $= 0.38\lambda$/cm, and GRMS $= 0.28\lambda$/cm. If we make our parameters better than these values, a small improvement in wavefront parameters could lead to a considerable improvement in performance. In a practical design, we should try our best to make our parameters better than these values. We assume a series of goals and list corresponding wavefront requirements in Table 2. It can be used as a design reference in the future.

We would like to discuss the changing trends of performance with some important parameters. First, in order to discuss the relationships between performance and pulse duration, pulse duration is set to 15, 20, and 30 fs, respectively. All the other parameters remain unchanged. By the methods discussed above, a series of fitted curves are plotted in Fig. 6. Data points have been hidden for convenience. The relationships among three evaluation indices of performance are shown in Figs. 6(a) and 6(b). Figures 6(c)–6(f) are the relationships between parameters of each beam's own wavefront and SR.

Most of the fitted curves are similar, which means that, for transform-limited ultrashort pulse coherent beam combining, requirements for each beam's own wavefront error are nearly the same as that for continuous wave coherent beam combining. However, for the case of small wavefront error, the requirements are slightly higher when we shorten the pulse duration. The reason is that the wavefront characteristics of different frequency components are similar in the focal plane for the transform-limited short pulse.

In some situations, we need to combine more than two channels. Therefore, it is valuable to discuss the relationships between requirements for each beam's own wavefront error and the number of channels. Shown as Fig. 7, the requirements are nearly the same and performance degenerates if we combine more channels in the case of small wavefront error.

The possible reason is that the influence of combining more channels is small. In the case of small wavefront error, the influence is more obvious. Combining more channels leads to

Table 2. Requirements for Each Beam's Own Wavefront Error Parameters Corresponding to Design Goals

	Requirements for Each Beam's Own Wavefront Error			
Goals	PV(λ)	RMS(λ)	GPV(λ/cm)	GRMS(λ/cm)
EC > 0.5	0.154	0.097	0.042	0.035
SR > 0.8	0.179	0.104	0.049	0.041
SRdl > 0.8	0.196	0.109	0.053	0.045

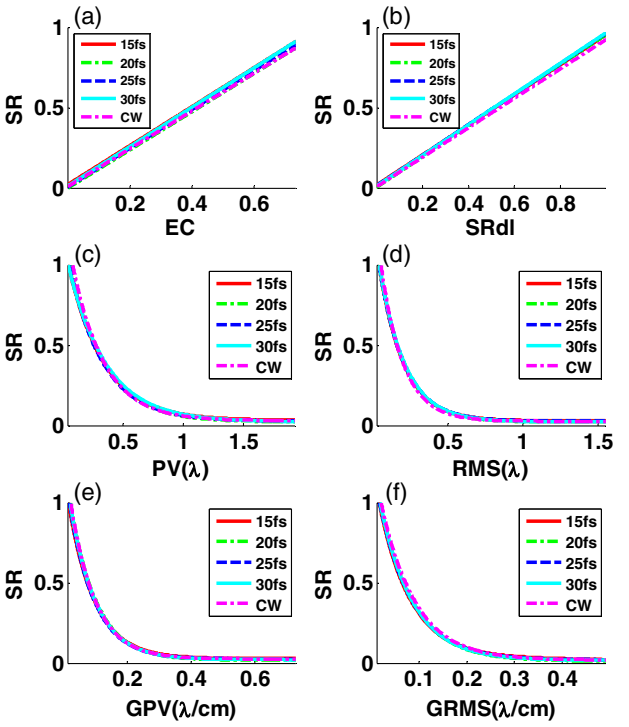

Fig. 6. (a)–(f) Relationships between each beam's own wavefront error and performance of combining for different pulse durations (CW represents continuous wave, and 15, 20, 25, and 30 fs are the pulse durations).

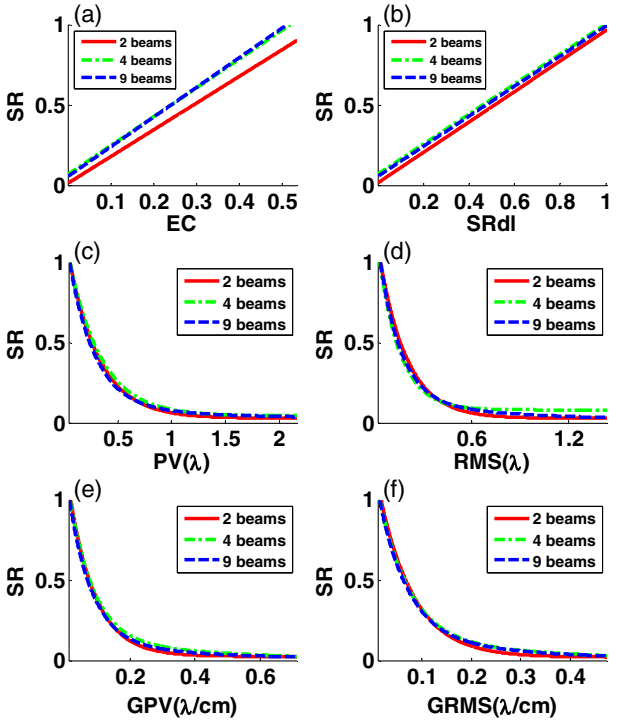

Fig. 7. (a)–(f) Relationships between each beam's own wavefront error and performance of combining for different numbers of channels.

the larger size of total aperture, and performance would degenerate if the wavefront error of each channel remains unchanged.

Combining more than two channels may be a good choice from the point of phase effects of coherent beam combining. The requirements will not change obviously and the higher peak power can be obtained in this situation.

4. REQUIREMENTS FOR THE DIFFERENCE AMONG BEAMS' WAVEFRONTS FOR LARGE-APERTURE ULTRASHORT LASER SYSTEMS COHERENT BEAM COMBINING

There are three kinds of differences among beams' wavefronts: piston, pointing (also known as tip/tilt), and a high-order difference among beams' wavefronts. All of these errors are discussed in Section 4.

A. Piston

Piston error could change far-field distribution dramatically due to the intrinsic nature of interference. There are many papers focusing on this topic [17,23,25–28]. However, most of the papers did not pay attention to the relationships between requirements for each beam's own wavefront and piston error. Since it is an important issue in large-aperture systems, some numerical simulations are carried out. The results are represented in Fig. 8.

The relationships between three evaluation indices of performance are shown as Figs. 8(a) and 8(b). Figures 8(c)–8(f) are the relationships between parameters of each beam's own wavefront and SR. The curves are fitted curves for different pistons. All the other parameters are set to the same as parameters in Section 3.

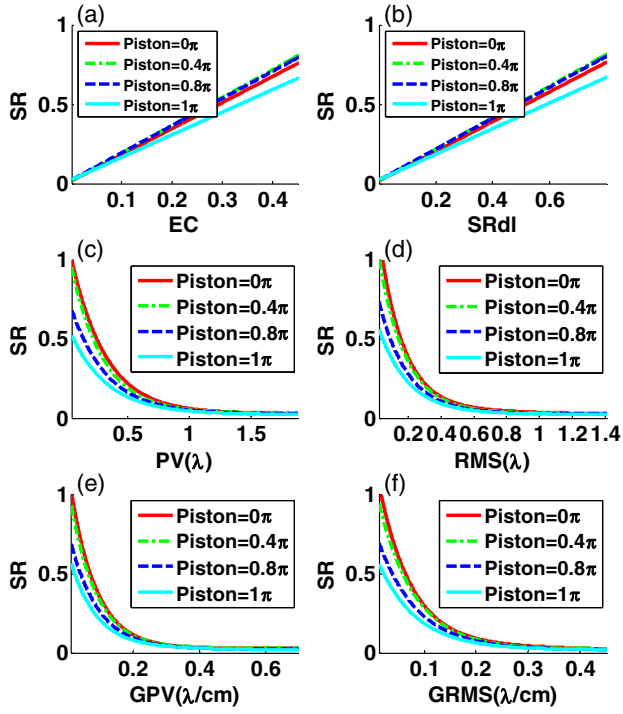

Fig. 8. (a)–(f) Relationships between each beam's own wavefront error and performance of combining for different piston.

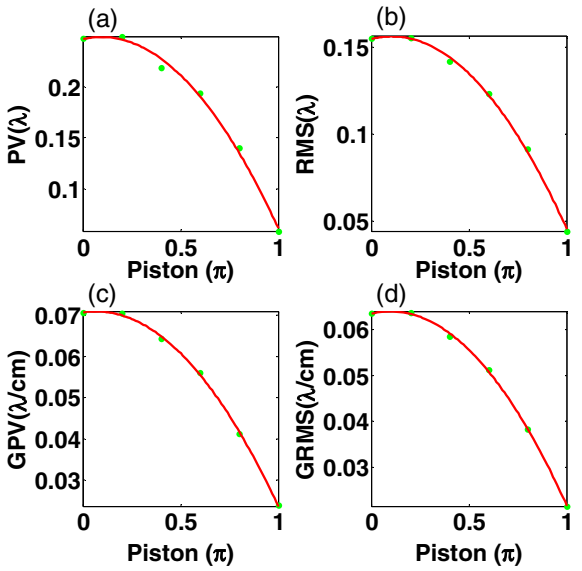

Fig. 9. (a)–(d) With SR > 0.5 as a goal, for example, relationships between the piston and requirements for each beam's own wavefront error.

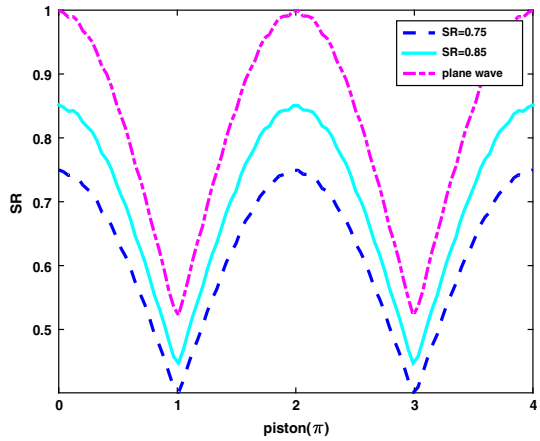

Fig. 10. Relationships between SR and the piston for different each beam's own wavefront error. (SR = 0.75, 0.85 refers to different values for each beam's own wavefront. When other errors equal zero, each beam's own wavefront decreases SR to the corresponding value. The plane wave refers to a perfectly flat wavefront.)

The changing trends of these curves are all similar. These curves converge to the same SR for different pistons when each beam's own wavefront error increases. It means that the piston does not affect the performance of combining markedly in the case of large wavefront error. For the case of small wavefront error, the piston affects the performance of combining considerably. We find that requirements become stricter when the piston error increases and that the maximum obtainable SR decreases due to the existence of the piston.

One reasonable explanation is that the piston would affect the intensity profile dramatically. It can lead to the degeneration of performance. This influence is obvious in the case of small wavefront error. However, in the case of large wavefront error, energy could not be focused on the focal point well. Peak intensity will be low and almost remain unchanged, even though the intensity profile has changed a lot due to piston error.

In the case of SR > 0.5, requirements for each beam's own wavefront error for different pistons are plotted in Fig. 9. The independent variable of Figs. 9(a)–9(d) is the piston and the dependent variables of Figs. 9(a)–9(d) are the requirements for PV, RMS, GPV, and GRMS corresponding to our performance goal, respectively.

We find that derivative of the wavefront requirements for a large piston is larger than that for a small piston. A possible reason is that the influence of the piston is not linear. A small piston is essential for a successful large-aperture coherent beam combining system. Relationships between SR and piston for different wavefronts are presented in Fig. 10. For large-aperture ultrashort laser systems coherent beam combining, SR exhibits similar periodic variations over the piston for different wavefront errors, and a larger wavefront error leads to a lower SR.

B. Pointing

Pointing error makes beams that can't overlap well. It is another important factor that degenerates the performance of combining [23,26,29,30]. However, most previous papers focus on the case of a small aperture. We would like to discuss the relationships between requirements for each beam's own wavefront and pointing error in large-aperture systems. There are two kinds of pointing error: tip and tilt. For simplicity, we do not draw on the results of the influence of tilt since they are similar to the results of the influence of tip. Our simulation results are represented in Fig. 11.

In Fig. 11, the meaning of the subgraphs are similar to their counterparts in Fig. 8. Curves are fitted curves for different tips. All the other parameters are set to the same parameters as in

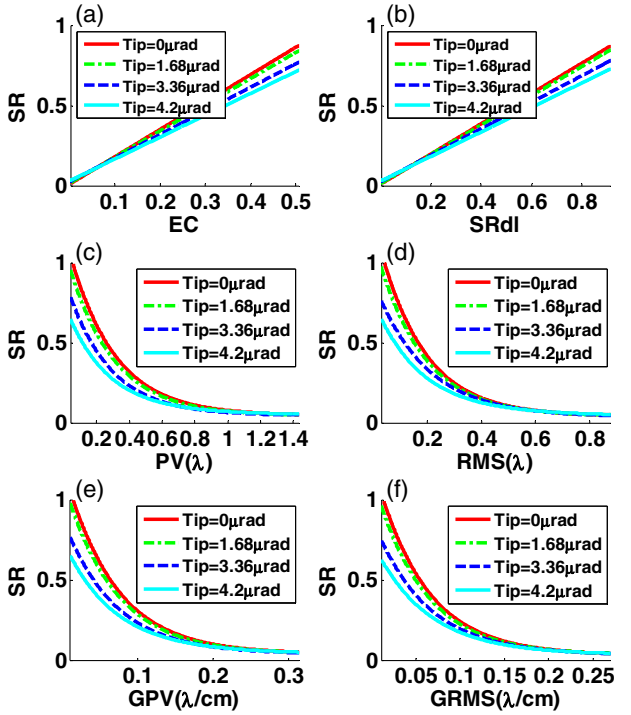

Fig. 11. (a)–(f) Relationships between each beam's own wavefront error and performance of combining for different tip.

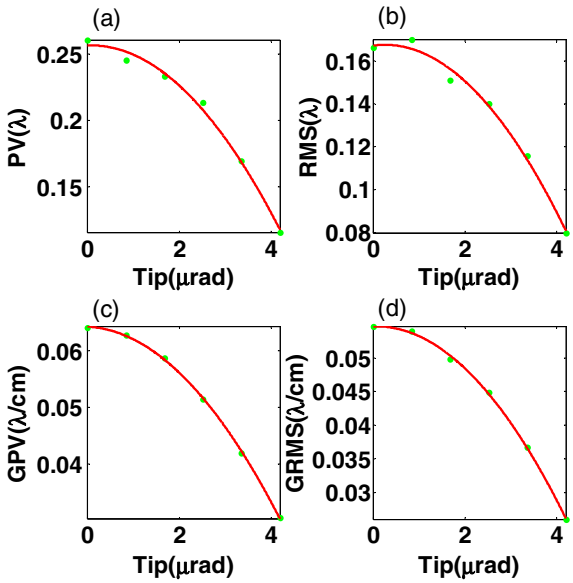

Fig. 12. (a)–(d) With SR > 0.5 as goal, for example, relationships between the tip and requirements for each beam's own wavefront error.

Section 3. We find that the influence of the pointing error is very similar to the influence of the piston. For the case of large wavefront error, the pointing error also has a small influence on performance. For the case of small wavefront error, the pointing error also affects performance considerably. The possible reason is similar to the reason in the discussion about influence of the piston.

In the case of SR > 0.5, requirements for each beam's own wavefront error for different tips are plot in Fig. 12. It is similar to the discussion of the piston. As shown in the figures, little pointing error has great influence on the performance in the case of small wavefront error. Besides, piston and pointing errors are usually easier to be corrected than each beam's own wavefront error. Therefore, for a practical system, we should first make piston and pointing errors as small as possible before correcting wavefront error. Relationships between SR and tip for different wavefronts are presented in Fig. 13. When each beam's own wavefront error becomes greater, the SR decreases quickly.

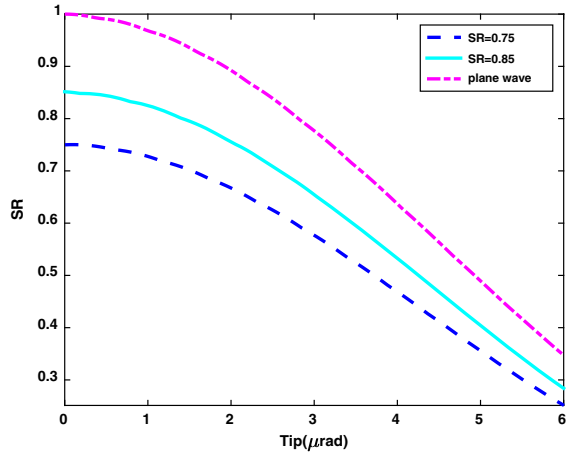

Fig. 13. Relationships between SR and tip for different each beam's own wavefront error (SR = 0.75, 0.85 refer to different values for each beam's own wavefront. When other errors equal zero, each beam's own wavefront decreases SR to the corresponding value. The plane wave refers to a perfectly flat wavefront.)

C. High-Order Difference among Beams' Wavefronts

In previous works, this topic has not been paid much attention, but it may be another important factor to decrease the performance of combining in large-aperture ultrashort laser systems. We assume that there are no piston and pointing errors in this section. To illustrate the meaning of this parameter, we plot Fig. 14. Figure 14(a) is the phase of channel A, which is one of the two channels used to build a coherent beam combining system. Figure 14(b) is the phase of channel B, which is another channel of a two-channel coherent beam combining system. Figure 14(c) is the phase difference of channel A and channel B. That phase difference is the physical meaning of the high-order difference among beams' wavefronts. According to the theory of interference, the high-order difference among beams' wavefronts also impact the far-field intensity distribution. For large-aperture systems, it may have a significant impact on performance.

In order to explain the physical meaning of our discussion more clearly, Figs. 15 and 16 are plotted. Figures 15(a)–15(d) are the wavefront of channel A, the wavefront of channel B, the phase difference of channel A and channel B, and the far-field intensity distribution, respectively, for the case of SR = 0.8. Figures 16(a)–16(d) show the corresponding results for the case of SR = 0.3.

In the latter case, the high-order difference among the beams' wavefronts is much greater than that in the former case. It results in degeneration of the far-field intensity distribution. Due to this degeneration, peak power and concentration of energy decrease considerably.

We use a similar approach to that discussed in Section 3, whereby variables are changed to parameters of the high-order difference among beams' wavefronts. Besides, we set each channel's phase to different phase screens in our discussion.

The simulation results are represented in Fig. 17 and they are similar to the results in Section 3. The meanings of the subgraphs are similar to their counterparts in Fig. 5. We find that

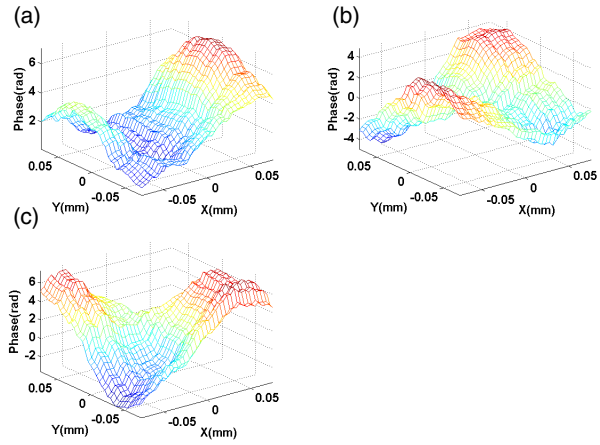

Fig. 14. Meaning of the high-order difference among beams' wavefronts. (a) Phase of channel A, (b) phase of channel B, and (c) phase difference of channel A and channel B.

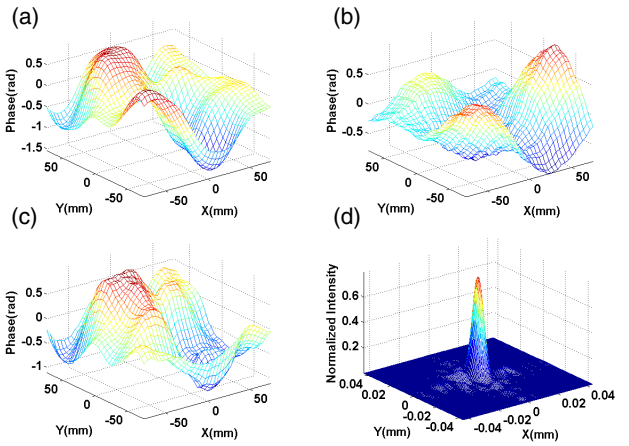

Fig. 15. (a), (b), (c), (d) Wavefront of channel A, wavefront of channel B, phase difference of channel A and channel B, and far-field intensity distribution, respectively, for the case of SR = 0.8.

the performance of combining increases rapidly if we make wavefront parameters better than certain values, too. The possible reason is that the small-wavefront-difference subaperture enlarges quickly when wavefront parameters are better than the certain values. Much higher peak powers can be obtained in this situation.

For this case, the values are about PV = 1.57λ, RMS = 1.19λ, GPV = 0.49λ/cm, and GRMS = 0.40λ/cm. We should try our best to meet these requirements. We also list requirements corresponding to different performance goals in Table 3, which would be useful to design a practical system.

In order to discuss the relationships between high-order differences among the beams' wavefronts and performance of combining for different pulse durations, the approach similar to that discussed in Section 3 is used. Our results are represented in Fig. 18. Figures 18(a) and 18(b) are the relationships between three evaluation indices of performance. Figures 18(c)–18(f) are the relationships between parameters of high-order difference among beams' wavefronts and SRs.

Shown as the fitted curves in Fig. 18, for transform-limited ultrashort pulse coherent beam combining, requirements for

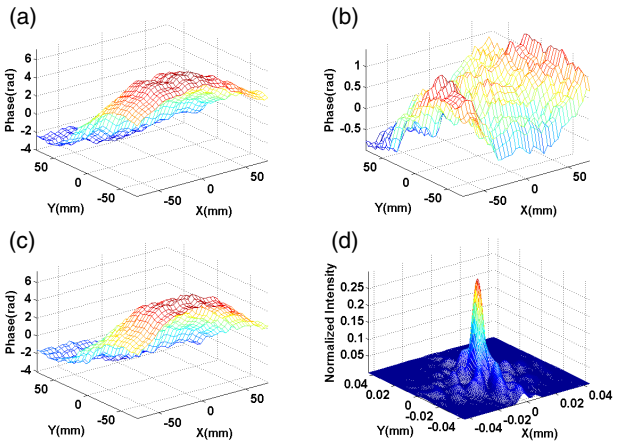

Fig. 16. (a), (b), (c), (d) Wavefront of channel A, wavefront of channel B, phase difference of channel A and channel B, and far-field intensity distribution, respectively, for the case of SR = 0.3.

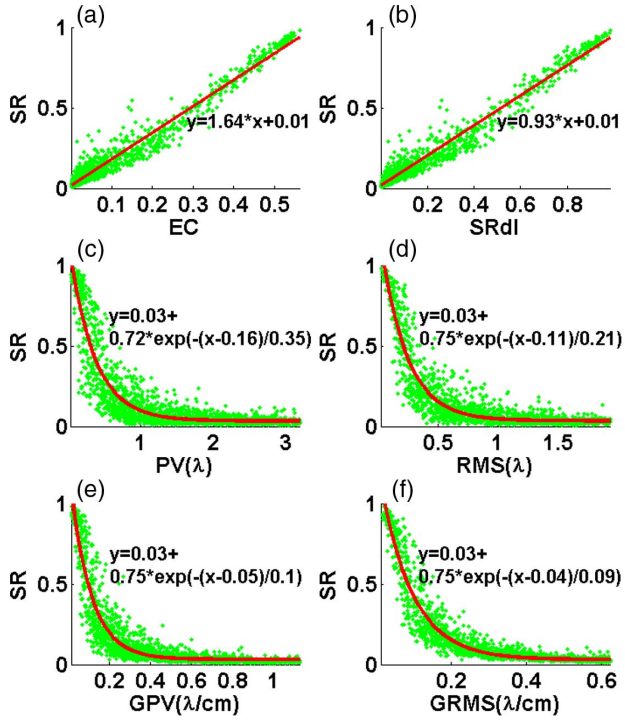

Fig. 17. (a)–(f) Effect of high-order difference among beams' wavefronts on two 25 fs transform-limited large-aperture coherent beam combining.

high-order differences among beams' wavefronts are the nearly same for different pulse durations. The reason may be that the wavefront characteristics of different frequency components are similar, which is the same as the discussion about the influence of each beam's own wavefront error. Pulse duration is not a key factor that affects requirements for high-order differences among beams' wavefronts.

Because there are more than two wavefront differences that can be used in the evaluation, in order to evaluate the performance in the case of combining more than two channels, we have to modify our evaluation method. First, the wavefront of two beams are set to a specific one. In our case, the specific wavefront makes SR equals to 0.8. We set one of the channels as the reference and the wavefront of this channel remains unchanged in our discussion. We change the wavefront of other channels randomly and use the mean of the difference between the wavefront of the reference channel and other channels as

Table 3. Requirements for the High-Order Difference among Beams' Wavefronts Corresponding to Design Goals

	Requirements for the High-Order Difference among Beams' Wavefronts			
Performance Goals	PV(λ)	RMS(λ)	GPV(λ/cm)	GRMS(λ/cm)
EC > 0.5	0.197	0.101	0.050	0.043
SR > 0.8	0.207	0.118	0.055	0.047
SRdl > 0.8	0.221	0.138	0.062	0.051

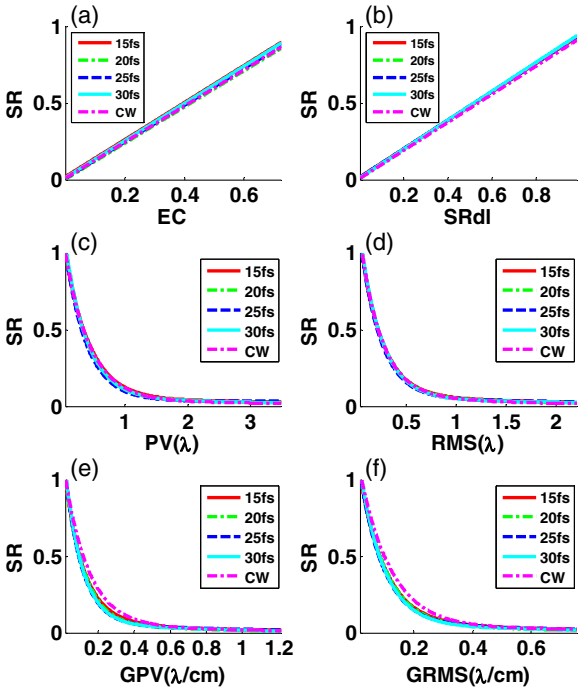

Fig. 18. (a)–(f) Relationships between high-order difference among beams' wavefronts and performance of combining for different pulse durations.

the evaluation index. Then, corresponding wavefront error parameters are calculated. Our results are represented in Fig. 19.

In the case of a small high-order wavefront difference, requirements for the mean high-order wavefront difference are similar since there is no difference between combining different numbers of channels in the case of a small wavefront error. Moreover, when the high-order wavefront difference increases, curves converge to different SRs, which become lower when combining more channels. The possible reason may be that more channels correspond to a larger total size of apertures and a greater possibility of destructive interference.

Taking into account the results in Section 3, combining more than two channels should be a good choice from the point of requirements for each beam's own wavefront error and requirements for the mean high-order wavefront difference. Requirements will not change obviously and higher peak powers can be obtained in this case.

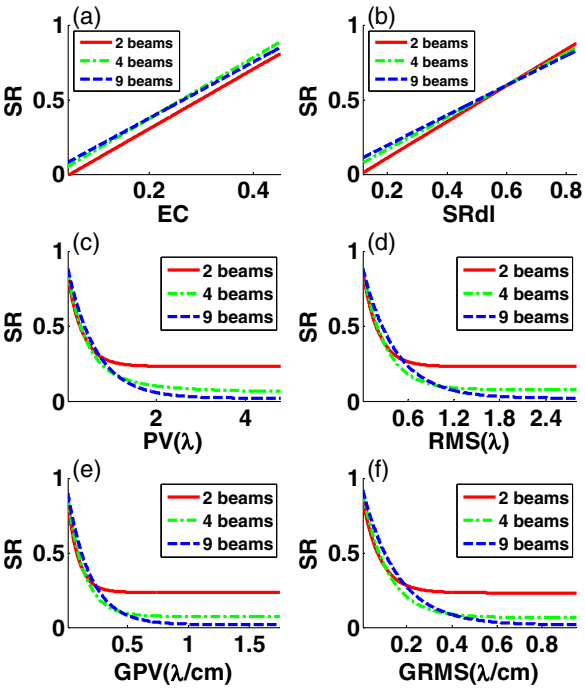

Fig. 19. (a)–(f) Relationships between the mean high-order wavefront difference and performance of combining for different numbers of channels (mean high-order wavefront difference refers to the mean of the wavefront difference between the reference and other channels).

5. CONCLUSION

In conclusion, this paper focuses on phase effects of large-aperture ultrashort laser systems coherent beam combining technology. A model is built to describe the coherent beam combining process for ultrashort pulses. With a series of numerical simulations, we obtain the requirements for phase parameters for an assumed two-channel large-aperture ultrashort laser system's coherent beam combining. Some changing trends of requirements for wavefront parameters are also presented. We find that the performance of combining increases rapidly if we make wavefront parameters better than certain values. For different pulse durations, the relationships are nearly same. Shorter pulse duration would not affect requirements for each beam's own wavefront error and high-order differences among beams' wavefronts significantly. In the case of combining more than two channels, we find that combining more than two channels should be a good choice from the point of requirements for each beam's own wavefront error and requirements for the mean high-order wavefront difference. Moreover, we find that piston and pointing errors have little influence on the performance of combining for the case of large wavefront error, but affects the performance of combining considerably for the case of small wavefront error. Higher piston or pointing error results in stricter requirements for each beam's own wavefront and smaller maximum obtainable SR. All of these works are helpful for designing a practical system in the near future to achieve unprecedented super-high peak powers.

Funding. National Natural Science Foundation of China (NSFC) (61205137).

REFERENCES

1. B. Rus, F. Batysta, J. Čáp, M. Divoký, M. Fibrich, M. Griffiths, R. Haley, T. Havlíček, M. Hlavác, J. Hřebíček, P. Homer, P. Hříbek, J. Jand'ourek, L. Juha, G. Korn, P. Korouš, M. Košelja, M. Kozlová, D. Kramer, M. Krůs, J. C. Lagron, J. Limpouch, L. MacFarlane, M. Malý, D. Margarone, P. Matlas, L. Mindl, J. Moravec, T. Mocek, J. Nejdl, J. Novák, V. Olšovcová, M. Palatka, J. P. Perin, M. Pešlo, J. Polan, J. Prokůpek, J. Řídký, K. Rohlena, V. Růžička, M. Sawicka, L. Scholzová, D. Snopek, P. Strkula, and L. Švéda, "Outline of the ELI-Beamlines facility," Proc. SPIE **8080**, 808010 (2011).
2. G. A. Mourou, T. Tajima, and S. V. Bulanov, "Optics in the relativistic regime," Rev. Mod. Phys. **78**, 309–371 (2006).
3. X. Liang, L. Yu, L. Xu, Y. Chu, Y. Xu, C. Wang, X. Lu, Y. Leng, R. Li, and Z. Xu, "Latest progress and research status of ultra-high intensity

lasers at SIOM," in *Advanced Solid State Lasers*, OSA Technical Digest (online) (Optical Society of America, 2014), paper AM1A.1.
4. Z. Liu, P. Zhou, X. Xu, X. Wang, and Y. Ma, "Coherent beam combining of high power fiber lasers: progress and prospect," Sci. China Technol. Sci. **56**, 1597–1606 (2013).
5. D. Strickland and G. Mourou, "Compression of amplified chirped optical pulses," Opt. Commun. **55**, 447–449 (1985).
6. A. Dubietis, G. Jonušauskas, and A. Piskarskas, "Powerful femtosecond pulse generation by chirped and stretched pulse parametric amplification in BBO crystal," Opt. Commun. **88**, 437–440 (1992).
7. V. Yanovsky, V. Chvykov, G. Kalinchenko, P. Rousseau, T. Planchon, T. Matsuoka, A. Maksimchuk, J. Nees, G. Cheriaux, G. Mourou, and K. Krushelnick, "Ultra-high intensity- 300-TW laser at 0.1 Hz repetition rate," Opt. Express **16**, 2109–2114 (2008).
8. A. Lyachev, O. Chekhlov, J. Collier, R. Clarke, M. Galimberti, C. Hernandez-Gomez, P. Matousek, I. Musgrave, D. Neely, P. Norreys, I. Ross, Y. Tang, T. Winstone, and B. Wyborn, "The 10PW OPCPA Vulcan laser upgrade," in *Advances in Optical Materials*, OSA Technical Digest (CD) (Optical Society of America, 2011), paper HThE2.
9. F. Giambruno, C. Radier, G. Rey, and G. Cheriaux, "Design of a 10 PW (150 J/15 fs) peak power laser system with Ti:sapphire medium through spectral control," Appl. Opt. **50**, 2617–2621 (2011).
10. A. Klenke, E. Seise, S. Demmler, J. Rothhardt, S. Breitkopf, J. Limpert, and A. Tünnermann, "Coherently-combined two channel femtosecond fiber CPA system producing 3 mJ pulse energy," Opt. Express **19**, 24280–24285 (2011).
11. M. Kienel, M. Muller, A. Klenke, T. Eidam, J. Limpert, and A. Tunnermann, "Experimental demonstration of multidimensional amplification of ultrashort pulses," Proc. SPIE **9344**, 934419 (2015).
12. B. Rus, P. Bakule, D. Kramer, G. Korn, J. T. Green, J. Nóvak, M. Fibrich, F. Batysta, J. Thoma, and J. Naylon, "ELI-Beamlines laser systems: status and design options," Proc. SPIE **8780**, 87801T (2013).
13. "Exawatt Center for Extreme Light Studies (XCELS), Project Summary," http://www.xcels.iapras.ru/img/site-XCELS.pdf.
14. S. Bagayev, V. Leshchenko, V. Trunov, E. Pestryakov, and S. Frolov, "Coherent combining of femtosecond pulses parametrically amplified in BBO crystals," Opt. Lett. **39**, 1517–1520 (2014).
15. V. E. Leshchenko, "Coherent combining efficiency in tiled and filled aperture approaches," Opt. Express **23**, 15944–15970 (2015).
16. A. Klenke, S. Breitkopf, M. Kienel, T. Gottschall, T. Eidam, S. Hadrich, J. Rothhardt, J. Limpert, and A. Tunnermann, "530 W, 1.3 mJ, four-channel coherently combined femtosecond fiber chirped-pulse amplification system," Opt. Lett. **38**, 2283–2285 (2013).
17. L. A. Siiman, W. Z. Chang, T. Zhou, and A. Galvanauskas, "Coherent femtosecond pulse combining of multiple parallel chirped pulse fiber amplifiers," Opt. Express **20**, 18097–18116 (2012).
18. V. E. Leshchenko, V. I. Trunov, S. A. Frolov, E. V. Pestryakov, V. A. Vasiliev, N. L. Kvashnin, and S. N. Bagayev, "Coherent combining of multimillijoule parametric-amplified femtosecond pulses," Laser Phys. Lett. **11**, 095301 (2014).
19. V. E. Leshchenko, V. A. Vasiliev, N. L. Kvashnin, and E. V. Pestryakov, "Coherent combining of relativistic-intensity femtosecond laser pulses," Appl. Phys. B **118**, 511–516 (2015).
20. S. N. Bagayev, V. I. Trunov, E. V. Pestryakov, S. A. Frolov, V. E. Leshchenko, A. E. Kokh, and V. A. Vasiliev, "Super-intense femtosecond multichannel laser system with coherent beam combining," Laser Phys. **24**, 074016 (2014).
21. S. N. Bagayev, V. I. Trunov, E. V. Pestryakov, V. E. Leschenko, S. A. Frolov, and V. A. Vasiliev, "High-intensity femtosecond laser systems based on coherent combining of optical fields," Opt. Spectrosc. **115**, 311–319 (2013).
22. H. Yuanxing, "Study of evaluating and measuring laser beam quality," Ph.D. thesis (National University of Defense Technology, 2012).
23. Y. Yang, "Study on coherent beam combination technology of high-energy short-pulse lasers," Ph.D. thesis (National University of Defense Science and Technology, 2011).
24. G. S. Fishman, *Monte Carlo* (Springer, 1996).
25. T. Weyrauch, M. A. Vorontsov, G. W. Carhart, L. A. Beresnev, A. P. Rostov, E. E. Polnau, and J. J. Liu, "Experimental demonstration of coherent beam combining over a 7 km propagation path," Opt. Lett. **36**, 4455–4457 (2011).
26. C. Geng, W. Luo, Y. Tan, H. Liu, J. Mu, and X. Li, "Experimental demonstration of using divergence cost-function in SPGD algorithm for coherent beam combining with tip/tilt control," Opt. Express **21**, 25045–25055 (2013).
27. Y. Zheng, X. Wang, F. Shen, and X. Li, "Generation of dark hollow beam via coherent combination based on adaptive optics," Opt. Express **18**, 26946–26958 (2010).
28. X. Wang, Q. Fu, F. Shen, and C. Rao, "Piston and tilt cophasing of segmented laser array using Shack–Hartmann sensor," Opt. Express **20**, 4663–4674 (2012).
29. X. Wang, X. Wang, P. Zhou, R. Su, C. Geng, X. Li, X. Xu, and B. Shu, "350-W coherent beam combining of fiber amplifiers with tilt-tip and phase-locking control," IEEE Photon. Technol. Lett. **24**, 1781–1784 (2012).
30. C. Geng, X.-Y. Li, X.-J. Zhang, and C.-H. Rao, "Influence and simulated correction of tip/tilt phase error on fiber laser coherent beam combination," Acta Phys. Sin. **60**, 114202 (2011).